Developmental Cell
Article

Integration of Kinase and Phosphatase Activities by BUBR1 Ensures Formation of Stable Kinetochore-Microtubule Attachments

Saskia J.E. Suijkerbuijk,[1] Mathijs Vleugel,[1] Antoinette Teixeira,[1] and Geert J.P.L. Kops[1,2,*]
[1]Molecular Cancer Research and Cancer Genomics Centre
[2]Department of Medical Oncology
UMC Utrecht, Universiteitsweg 100, 3584 CG Utrecht, The Netherlands
*Correspondence: g.j.p.l.kops@umcutrecht.nl
http://dx.doi.org/10.1016/j.devcel.2012.09.005

SUMMARY

Maintenance of chromosomal stability depends on error-free chromosome segregation. The pseudokinase BUBR1 is essential for this, because it is a core component of the mitotic checkpoint and is required for formation of stable kinetochore-microtubule attachments. We have identified a conserved and highly phosphorylated domain (KARD) in BUBR1 that is crucial for formation of kinetochore-microtubule attachments. Deletion of this domain or prevention of its phosphorylation abolishes formation of kinetochore microtubules, which can be reverted by inhibiting Aurora B activity. Phosphorylation of KARD by PLK1 promotes direct interaction of BUBR1 with the PP2A-B56α phosphatase that counters excessive Aurora B activity at kinetochores. As a result, removal of BUBR1 from mitotic cells or inhibition of PLK1 reduces PP2A-B56α kinetochore binding and elevates phosphorylation of Aurora B substrates on the outer kinetochore. We propose that PLK1 and BUBR1 cooperate to stabilize kinetochore-microtubule interactions by regulating PP2A-B56α-mediated dephosphorylation of Aurora B substrates at the kinetochore-microtubule interface.

INTRODUCTION

Formation and subsequent stabilization of kinetochore-microtubule interactions requires a balance of counteracting kinase and phosphatase activities. The principal kinase that destabilizes erroneous interactions is Aurora B. Phosphorylation of the microtubule-binding KNL1/MIS12/NDC80 complex (KMN) network by Aurora B decreases the affinity of the KMN network for microtubules (Cheeseman et al., 2006; DeLuca et al., 2006; Wei et al., 2007; Welburn et al., 2010), thus allowing error correction to occur. Chromosome biorientation spatially removes KMN network substrates from inner-centromere-localized Aurora B (Liu et al., 2009), while initiating dephosphorylation of these substrates by promoting kinetochore binding of PP1γ (Liu et al., 2010). Prior to biorientation, however, initial kinetochore-microtubule interactions are protected from premature destabilization by Aurora B, and a recent study showed that this is ensured by the binding of the PP2A-B56α phosphatase to prometaphase kinetochores (Foley et al., 2011). Formation of stable interactions between kinetochores and microtubules further depends on PLK1 (Foley et al., 2011; Lénárt et al., 2007; Sumara et al., 2004; van Vugt et al., 2004) and the pseudokinase BUBR1 (Ditchfield et al., 2003; Lampson and Kapoor, 2005; Suijkerbuijk et al., 2012) that impinge on the Aurora B network via unknown mechanisms. Here we show that PLK1 and BUBR1 cooperate to stabilize kinetochore-microtubule interactions. We have identified a small conserved domain in BUBR1 that is essential for kinetochore-microtubule attachment. This domain is phosphorylated by PLK1 and recruits the Aurora B counteracting phosphatase PP2A-B56α to regulate kinetochore-microtubule attachments.

RESULTS

Identification of a Motif in BUBR1 Required for Formation of Stable Kinetochore-Microtubule Attachments

We and others have previously shown that an amino-terminal fragment of BUBR1 encompassing the TPR domain, two KEN boxes, and the BUB3-binding GLEBS motif (1–483 of human BUBR1) is capable of sustaining a mitotic checkpoint but cannot support kinetochore-microtubule attachments and therefore does not allow chromosome alignment (Malureanu et al., 2009; Suijkerbuijk et al., 2010) (Figure 1A). Chromosome alignment was restored in BUBR1-depleted cells by expression of a truncated protein that lacks only the carboxy-terminal kinase domain (731X), which implies that the attachment function of BUBR1 is independent of the pseudokinase domain and resides in the sequence between 483 and 731 (Suijkerbuijk et al., 2010; Figures 1A and 1C). To further pinpoint the region within BUBR1 that supports attachments, a panel of truncation mutants was analyzed for ability to restore BUBR1 function in a small hairpin RNA (shRNA)-based reconstitution system (Suijkerbuijk et al., 2010) (Figures 1B and 1C). Chromosome alignment was assessed in BUBR1-depleted cells expressing various shRNA-resistant mutants and treated with the proteasome inhibitor MG132 to prevent mitotic exit. BUBR1-715X and -731X, but not -580X and -665X, supported efficient chromosome alignment and could thus replace endogenous BUBR1 (Figure 1C). BUBR1 sequences proximal to the pseudokinase domain (amino

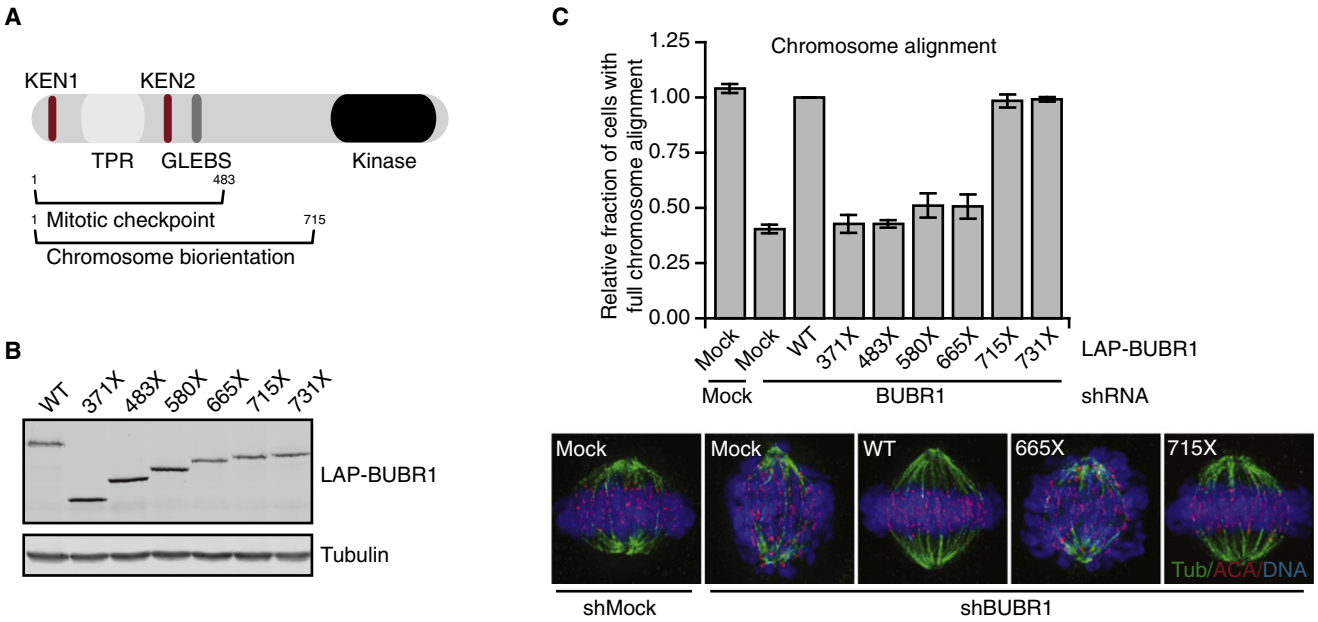

Figure 1. Kinase-Proximal Sequences in BUBR1 Are Required for Chromosome Alignment

(A) Schematic representation of domain architecture of BUBR1. The contribution of the sequences for BUBR1 function is indicated below, numbers indicate amino acid position.

(B) GFP and tubulin immunoblots of lysates of U2OS cells transfected with wild-type or mutant LAP-BUBR1.

(C) Chromosome alignment in HeLa cells transfected with indicated shRNAs in combination with RNAi-insensitive LAP-tagged BUBR1, treated with MG132 for 60 min, and immunostained for tubulin and centromeres (ACA). Representative images are shown and graph represents the relative fraction of cells with full chromosome alignment (average of four experiments, ±SEM).

acid 665–715) therefore harbor a functional region that is essential for chromosome alignment (Figure 1C). Within this region, 665–682 displayed high sequence conservation in animal BUBR1 homologs (Figure 2A). Removal of this region, hereafter referred to as the Kinetochore Attachment Regulatory Domain (KARD), abolished chromosome alignment (Figure 2B, ΔKARD).

Multisite Phosphorylation Is Essential for Function of the KARD Motif

The KARD contains four serine/threonine residues, three of which are relatively well conserved (S670, S676, and T680; Figure 2A). Of these, S670 and S676 have been reported to be phosphorylated in mitosis, either in response to lack of attachment (pS670 [Elowe et al., 2010; Huang et al., 2008]) or lack of tension (pS676 [Elowe et al., 2007]). Although no function was assigned to pS676 (Elowe et al., 2007), inhibiting S670 phosphorylation slightly reduced the efficiency of chromosome biorientation (Huang et al., 2008). To examine potential contribution of these three conserved residues to KARD function, chromosome alignment was examined in BUBR1-depleted cells expressing BUBR1 proteins carrying alanine substitutions at positions 670, 676, or 680. Cells expressing either of the single substitution mutants exhibited a relatively minor defect in chromosome alignment (Figure 2B). In contrast, substituting all three residues simultaneously (BUBR1-3A) abolished chromosome alignment to the same extent as BUBR1 depletion (Figure 2B). Analysis of cold-stable microtubules showed that cells expressing BUBR1-ΔKARD or BUBR1-3A were unable to form stable kinetochore-microtubule attachments (Figure 2C), as previously reported for BUBR1 depletion (Lampson and Kapoor, 2005). This was not due to inability of these proteins to accumulate at unattached kinetochores (Figure 2D). Importantly, replacement of S670, S676, and T680 by phosphomimetic aspartic acid residues (BUBR1-3D) fully restored chromosome alignment and formation of stable kinetochore attachments in BUBR1-depleted cells (Figures 2B and 2C). This strongly supports the hypothesis that the attachment defects observed with expression of BUBR1-3A were due to lack of phosphorylation of these residues.

Phosphorylation of T680 by PLK1 Is Essential for KARD Function

Mutational analysis of the three residues showed that the most severe effect on chromosome alignment was caused by substitution of T680 (Figure 2B). To determine whether T680 was phosphorylated in vivo, we generated a phosphospecific antibody to detect pT680 in cells. pT680-positive kinetochores were evident in prometaphase cells, as well as in nocodazole treated cells (Figures 3A and 3D). The antibody specifically detected pT680-BUBR1, as it could neither detect kinetochores in BUBR1-depleted cells (see siBUBR1 images and quantification in Figures 4C–4E), nor recognize immunoprecipitated BUBR1-T680A or λ phosphatase-treated BUBR1-WT (Figure 3B). Interestingly, BUBR1-positive kinetochores in prophase cells exhibited low pT680-BUBR1 signal, indicating that phosphorylation of this epitope occurs after nuclear envelope breakdown (Figure 3A). Furthermore, all kinetochores in taxol- or S-trityl-L-cysteine (STLC)-treated cells were recognized by

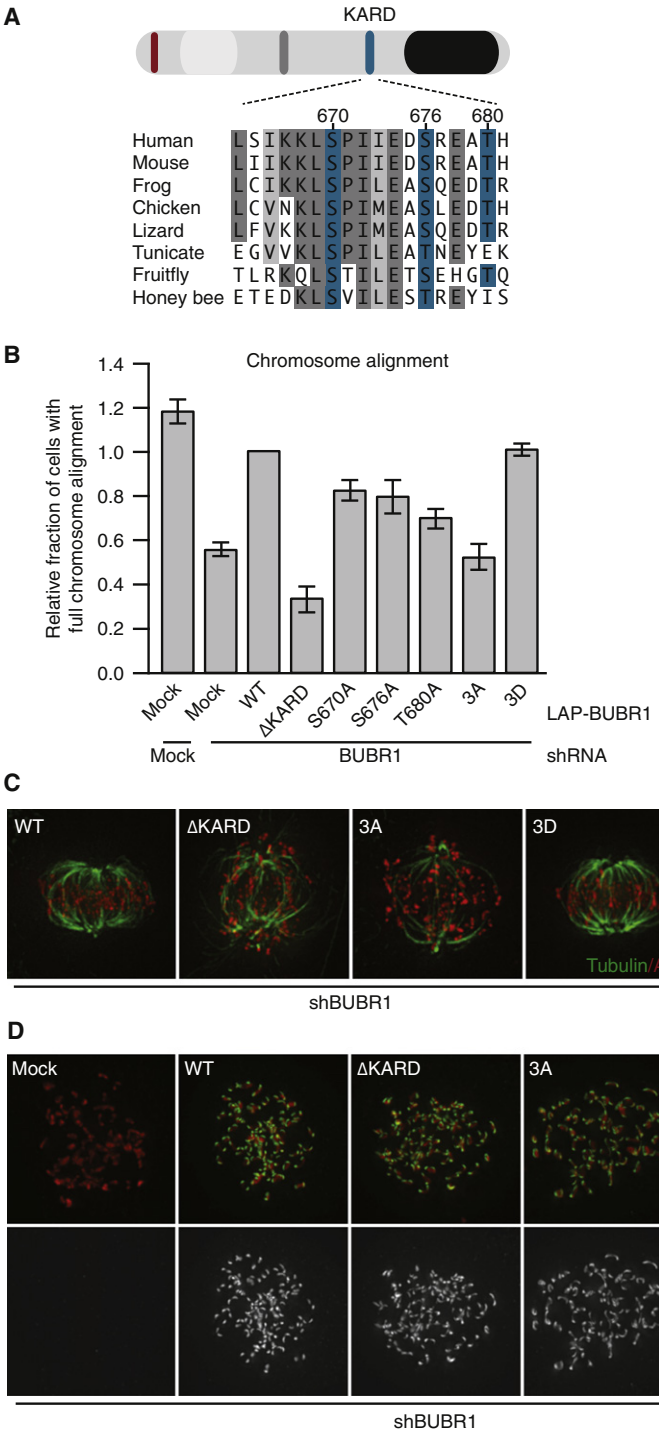

Figure 2. KARD, a Conserved and Highly Phosphorylated Domain in BUBR1, Is Essential for Kinetochore-Microtubule Attachment

(A) Schematic representation of domain architecture of BUBR1 and sequence alignment of the Kinetochore Attachment and Regulatory Domain (KARD). Conserved (gray) and phosphorylated (blue) residues are indicated, numbers indicate the position based on the sequence of human BUBR1. Human, *Homo sapiens*; mouse, *Mus musculus*; frog, *Xenopus tropicalis*; chicken, *Gallus gallus*; lizard; *Anolis carolinensis*; tunicate, *Ciona intestinalis*; fruitfly, *Drosophila melanogaster*; honey bee, *Apis mellifera*.

(B) Chromosome alignment in HeLa cells transfected with indicated shRNAs in combination with RNAi-insensitive LAP-tagged BUBR1 and treated with MG132 for 90 min. Graph represents the relative fraction of cells with full chromosome alignment (±SEM).

(C) Cold-stable microtubules in HeLa cells transfected as in (B), treated with MG132 for 60 min and immunostained for tubulin and centromeres (ACA).

(D) BUBR1 localization in HeLa cells transfected as in (B) and treated with nocodazole and MG132 for 30 min and immunostained for GFP and centromeres (ACA).

the pT680 antibody (Figures 3D and 3E). Since in these cells only few kinetochores are expected to be unattached but all will have low tension between sisters (Kapoor et al., 2000; Waters et al., 1998), this indicates that phosphorylation of T680 is independent of attachment status and may correlate with lack of interkinetochore tension. This is further supported by our observation that immunopurified BUBR1 was found phosphorylated on T680 to equal extents in cells in which the amount of unattached kinetochore differed but in which all sister kinetochores were at low tension (nocodazole versus taxol and STLC) (Figure 3C). Nevertheless, a thorough interrogation of pT680 and BUBR1 levels in relation to the distance between individual sister kinetochores will be required to conclusively show that pT680 is tension sensitive.

Phosphorylation of T680 behaved similar to that of S676-BUBR1, which is phosphorylated by PLK1 on tension-less kinetochores (Elowe et al., 2007). As T680 lies in a sequence that resembles the PLK1 consensus motif D/E-x-S/T-Φ-x-D/E (E-A-T-H-S-S; Alexander et al., 2011; Nakajima et al., 2003), where one or both of the serine residues may be phosphorylated), we next addressed whether this site is phosphorylated by PLK1. Recombinant active (WT) but not kinase-dead (K82R) PLK1 was able to phosphorylate LAP-BUBR1 on T680 in vitro (Figure 4A). This could be prevented by addition of the small molecule PLK1 inhibitor BI2536 (Lénárt et al., 2007) and was strongly reduced by mutation of T680 to alanine (T680A) (Figure 4A). Residual pT680 signal on in vitro phosphorylated T680A-BUBR1 was likely an in vitro artifact, since the pT680 antibody did not recognize T680A in cells (Figure 3B). Importantly, inhibition of PLK1 in cells by treatment with BI2536 greatly reduced staining of pT680 on unattached kinetochore as well

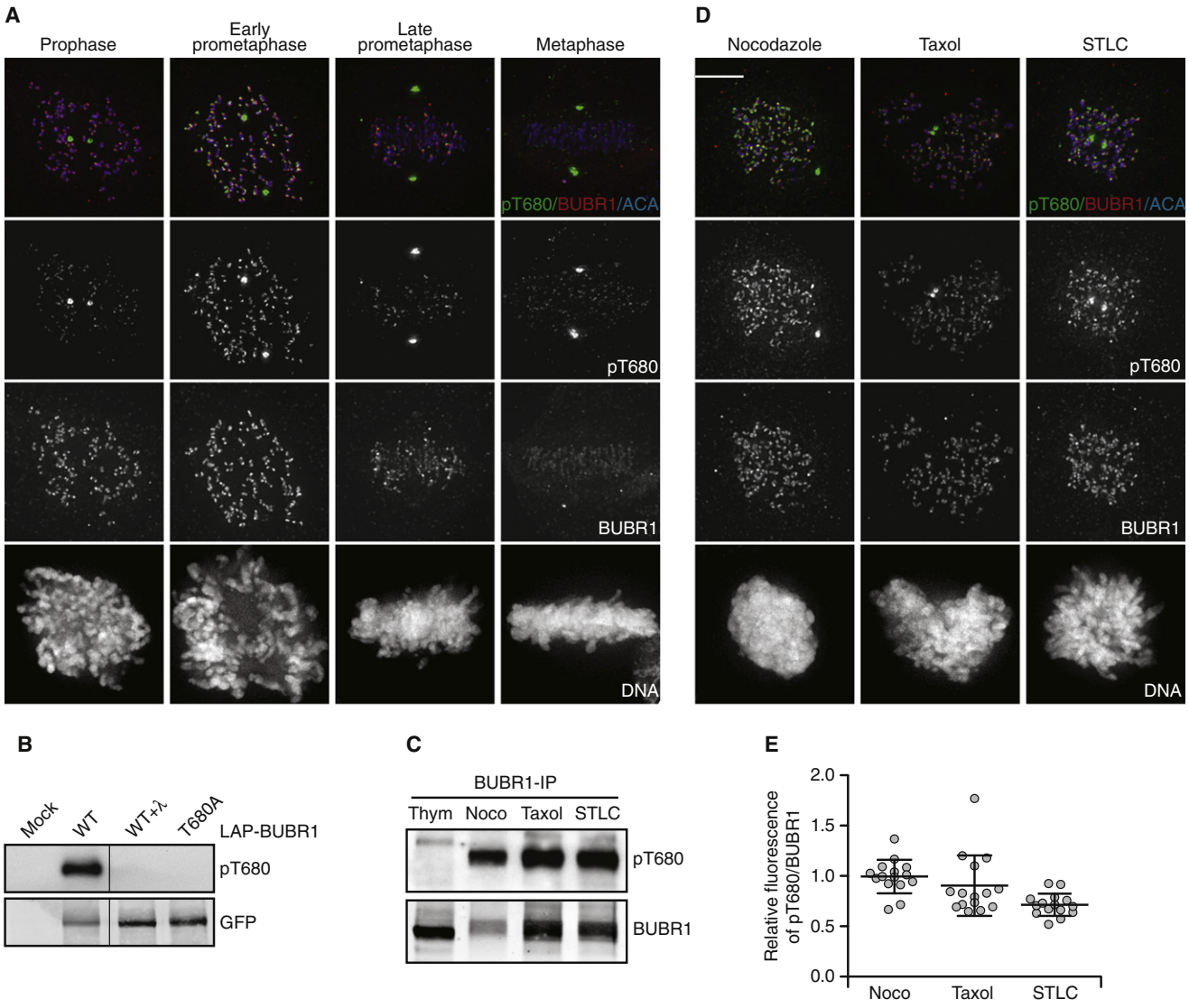

Figure 3. The KARD Is Phosphorylated on T680 in Cells

(A, D, and E) pT680 localization in unperturbed HeLa cells (A) or in HeLa cells treated with the indicated compounds for 1 hr (B) and immunostained for pT680, BUBR1 and centromeres (ACA). Graphs in (E) represent total kinetochore intensity of pT680 relative to BUBR1, ±SD.

(B) pT680 and GFP immunoblot of purified LAP-BUBR1 (WT or T680A) from mitotic HeLa cells, mock or λ phosphatase treated for 30 min after purification.

(C) pT680 and BUBR1 immunoblot of immunopurified BUBR1 from mitotic HeLa cells treated as indicated.

as on immunoprecipitated BUBR1 (Figures 4B–4E). Together, these data show that pT680 is a functionally relevant, PLK1-dependent phosphorylation on BUBR1. Furthermore, pT680 is part of a cluster of three attachment- and tension-sensitive phosphorylation sites that together are responsible for the formation of kinetochore-microtubule attachments (Elowe et al., 2007, 2010; Huang et al., 2008).

BUBR1 via Its KARD Recruits PP2A-B56α to Kinetochores

We next asked how the KARD and phosphosites therein might promote kinetochore-microtubule attachments. A yeast-2-hybrid screen with the carboxy-terminal 511 amino acids of BUBR1 (aa 540–1050) was performed on a cDNA library of human breast tumor epithelial cells. High- or medium-confidence interactors included Anillin, UBR4, CAMGAP1, AKR1B1, and many clones of various isoforms of the B56 regulatory subunit of the phosphatase PP2A, most notably B56α and B56γ (Figure 5A). B56δ and B56ε isoforms were also identified, albeit with lower confidence scores (Figure 5A). The PP2A holoenzyme is a trimeric complex consisting of a core of the catalytic C and scaffold A subunits, together with a variable regulatory B subunit that determines specificity (Janssens and Goris, 2001). PP2A-B56 was recently reported as a kinetochore-bound, tension-sensitive phosphatase that is required for formation of stable kinetochore-microtubule interactions by balancing Aurora B activity in prometaphase (Foley et al., 2011). The interaction between BUBR1 and PP2A-B56α was confirmed by coprecipitation of HA-PP2A-B56α with LAP-BUBR1 from mitotic cell lysates

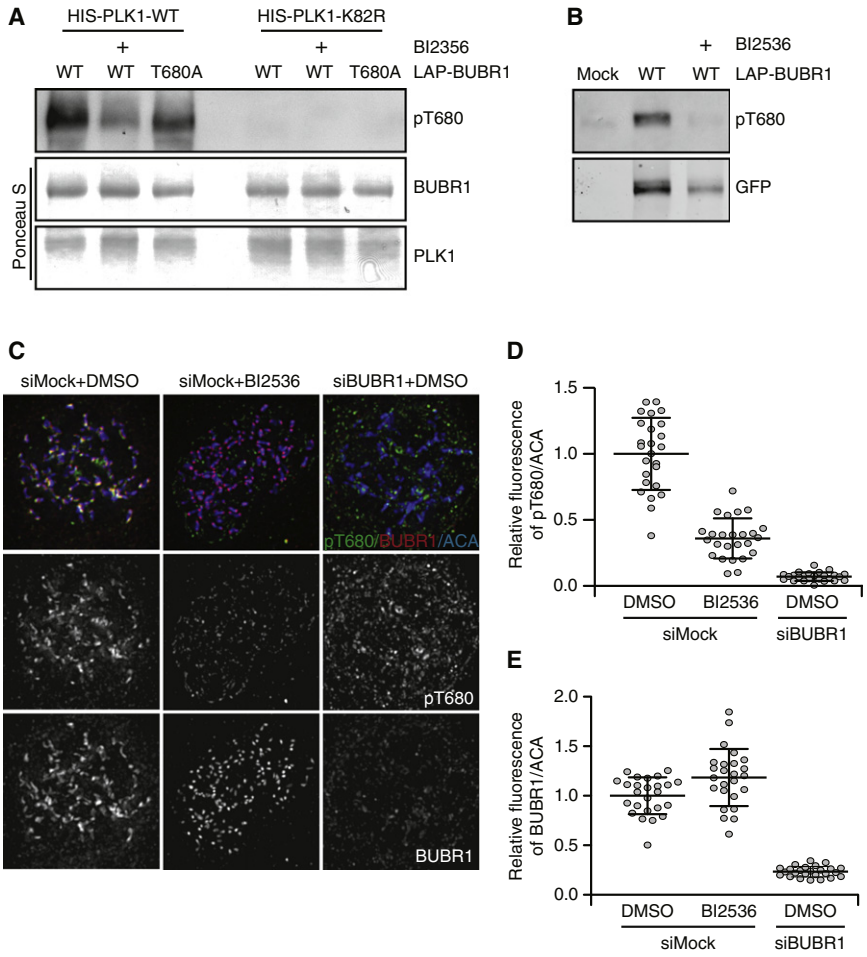

Figure 4. PLK1 Phosphorylates BUBR1-T680 In Vitro and in Cells

(A) In vitro kinase assay of PLK1 (WT or K82R) toward LAP-BUBR1 (WT or T680A) pT680, in the presence of DMSO or BI2536 (100 nM). Immunoblot of pT680-BUBR1 and total protein levels are shown.

(B) pT680 and GFP immunoblot of purified LAP-BUBR1 purified from mitotic HeLa cells treated with BI2536 or DMSO for 1 hr.

(C–E) pT680 immunolocalization in HeLa cells transfected with indicated siRNAs, treated as indicated combined with nocodazole and MG132 for 30 min, and immunostained for BUBR1, pT680, and centromeres (ACA). Representative images are shown (C). Graphs (D and E) represent total kinetochore intensity of pT680 (D) and BUBR1 (E) relative to centromeres (ACA), ±SD.

(Figure 5B). Binding of B56α to BUBR1 was dependent on the KARD, as the interaction was strongly reduced when the KARD was deleted (BUBR1-ΔKARD) (Figure 5B). Furthermore, mutation of the KARD (BUBR1-3A) as well as inhibition of PLK1 using BI2536 diminished the BUBR1-PP2A interaction, while phosphomimetic mutations of the three KARD residues (BUBR1-3D) rendered the interaction insensitive to PLK1 inhibition (Figure 5B). We thus conclude that PLK1-dependent phosphorylation of the three amino acid cluster in the KARD is essential for the BUBR1-B56α interaction. To more directly examine the interaction between BUBR1 and PP2A-B56α in cells, we asked whether a BUBR1 protein that is localized to ectopic foci could recruit PP2A-B56α to those sites. Importantly, expression of BUBR1 fused to the Lac repressor protein (LacI-LAP-BUBR1) in cells containing a stably integrated tandem Lac-operator (LacO) array (Janicki et al., 2004) resulted in recruitment of HA-PP2A-B56α to these foci (Figure 5C). No binding of HA-PP2A-B56α to LacI-LAP foci was observed, indicating that this localization is specific to the interaction with BUBR1. Recruitment of PP2A-B56α to the LacO foci was dependent on the phosphorylated KARD domain within the LacI-BUBR1 protein: deletion of the domain, mutation of the phosphorylated residues, or treatment with BI2536 greatly reduced the number of cells with PP2A-B56α-positive foci (Figures 5C and 5D). The ability of LacI-BUBR1 to recruit PP2A-B56α became independent of PLK1 activity when the KARD contained phosphomimetic residues (Figure 5D). Together these data indicate that PLK1-dependent phosphorylations in the KARD domain promote direct interaction between BUBR1 and PP2A-B56α.

KARD-Dependent Recruitment of PP2A Promotes Stable Kinetochore-Microtubule Interactions by Balancing Aurora B Activity

Removal of PP2A-B56 from cells causes defects in kinetochore-microtubule attachments in mitosis similar to those seen after removal of BUBR1 (Foley et al., 2011). We therefore asked whether BUBR1 is required for PP2A-B56α function at kinetochores. Indeed, localization of the phosphatase to kinetochores of unattached chromosomes was reduced in cells depleted of BUBR1 as well as in cells treated with the PLK1 inhibitor BI2536 (Figures 6A and 6B). Residual PP2A-B56α at kinetochores may be due to incomplete depletion of BUBR1 or, alternatively, to BUBR1-independent pools of PP2A-B56α such as one that is associated with SGO1 and that protects sister-centromere cohesion (Kitajima et al., 2006; Riedel et al., 2006; Tang et al., 2006). Importantly, depletion of BUBR1 correlated with increased phosphorylation of S109 on DSN1, an Aurora B-dependent modification that negatively impacts affinity of the KMN network for microtubules (Welburn et al., 2010) (Figures 6C and 6D). This was similar to reductions in DSN1 phosphorylation upon depletion of PP2A-B56 (Foley et al., 2011). To examine whether the BUBR1-PP2A-B56α interaction regulated stability of kinetochore-microtubule interactions by balancing Aurora B activity at kinetochores, cells expressing various BUBR1 mutants were treated with the Aurora B inhibitor ZM447439 (Ditchfield et al., 2003). Inspection of the interactions between kinetochores and cold-stable microtubules revealed that the majority of kinetochores in cells expressing BUBR1-ΔKARD and BUBR1-3A and treated with

A

Gene	# Clones	Confidence
PP2A-B56α	23	Very High
UBR4	22	Very High
Anillin	13	Very High
AKR1B1	10	Good
ARHGAP27	9	Good
PP2A-B56γ	2	Good
DDX11	4	Moderate
RNF103	4	Moderate
CENPE	1	Moderate
HYOU1	1	Moderate
MCM7	1	Moderate
NOTCH3	1	Moderate
PP2A-B56δ	1	Moderate
PPL	1	Moderate
PRP4	1	Moderate
RFXDC2	1	Moderate
RNF103	1	Moderate
SOX12	1	Moderate
UNK	1	Moderate
VPS13A	1	Moderate
PP2A-B56ε	13	Low

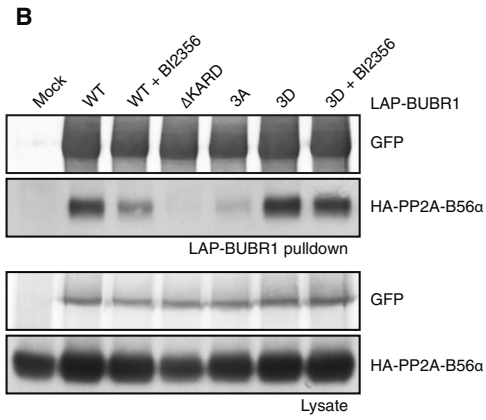

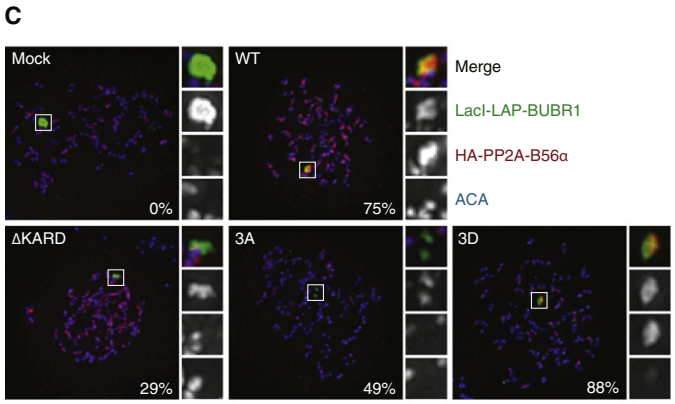

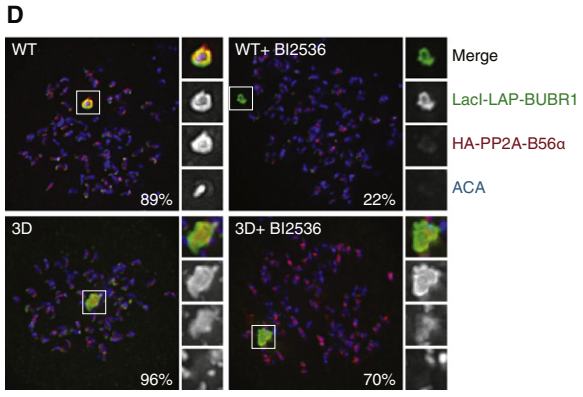

Figure 5. Phosphorylation-Dependent Interaction between BUBR1-KARD and PP2A-B56α

(A) Table summarizing interactions with BUBR1 identified by yeast two-hybrid. Regulatory PP2A-B56 subunits are shown in gray.

(B) BUBR1 (GFP) and PP2A-B56α (HA) immunoblots of cell lysates (lower) or immunopurified BUBR1 (wild-type and indicated mutants) (upper) of mitotic HEK 293T cells coexpressing HA-PP2A-B56α and LAP-BUBR1 and treated with BI2536 or DMSO for 1 hr.

(C and D) Immunolocalization of LacI-LAP-BUBR1 variants (anti-GFP), HA-PP2A-B56α (anti-HA) and centromeres (ACA) in nocodazole-treated U2OS LacO cells. BI2536 was added when indicated (D) Representative images are shown, the insets display LacO foci. Percentages of LacI-LAP-BUBR1-positive foci that costained with HA-PP2A-B56α are indicated (average of at least 50 cells).

DMSO and MG132 for 2 hr were unattached (Figure 6E). Strikingly, addition of ZM447439 during the final hour of treatment caused formation of stable attachments in both BUBR1-ΔKARD and BUBR1-3A-expressing cells. Thus, Aurora B activity was the principal cause of the weak kinetochore-microtubule interactions in these cells.

The data presented thus far favor the hypothesis that stabilization of kinetochore-microtubule attachments by BUBR1 is due to phospho-KARD-dependent recruitment of PP2A that balances excessive Aurora B activity toward the KMN network. If this is a major mechanism by which BUBR1 contributes to kinetochore-microtubule attachments, BUBR1 should become dispensable when PP2A is localized to outer kinetochores in a BUBR1-independent manner. To test this, the region of BUBR1 spanning the KARD domain (aa 647–697) was constitutively localized to kinetochores by fusion to the MIS12 protein (Jelluma et al., 2010; Maldonado and Kapoor, 2011) (Figure 7A). A wild-type version of the KARD could not restore chromosome alignment in BUBR1-depleted cells (Figures 7B and 7C), as it is likely unphosphorylated due to the absence of the priming T620 residue required for phosphorylation by PLK1 (Elowe et al., 2007). Strikingly, however, the KARD carrying phosphomimetic mutations (MIS12-KARD-3D) but not phospho-dead mutations (MIS12-KARD-3A) fully rescued chromosome alignment in the absence of BUBR1 (Figures 7B and 7C). We thus conclude that the phosphorylated KARD is the predominant mediator for stabilization of kinetochore-microtubule attachments by BUBR1.

DISCUSSION

The data presented here show that multisite phosphorylation of BUBR1 in the KARD regulates the balance of Aurora B activity at kinetochores by recruitment of PP2A-B56α (Figure 7D). Two functionally important sites within the KARD are

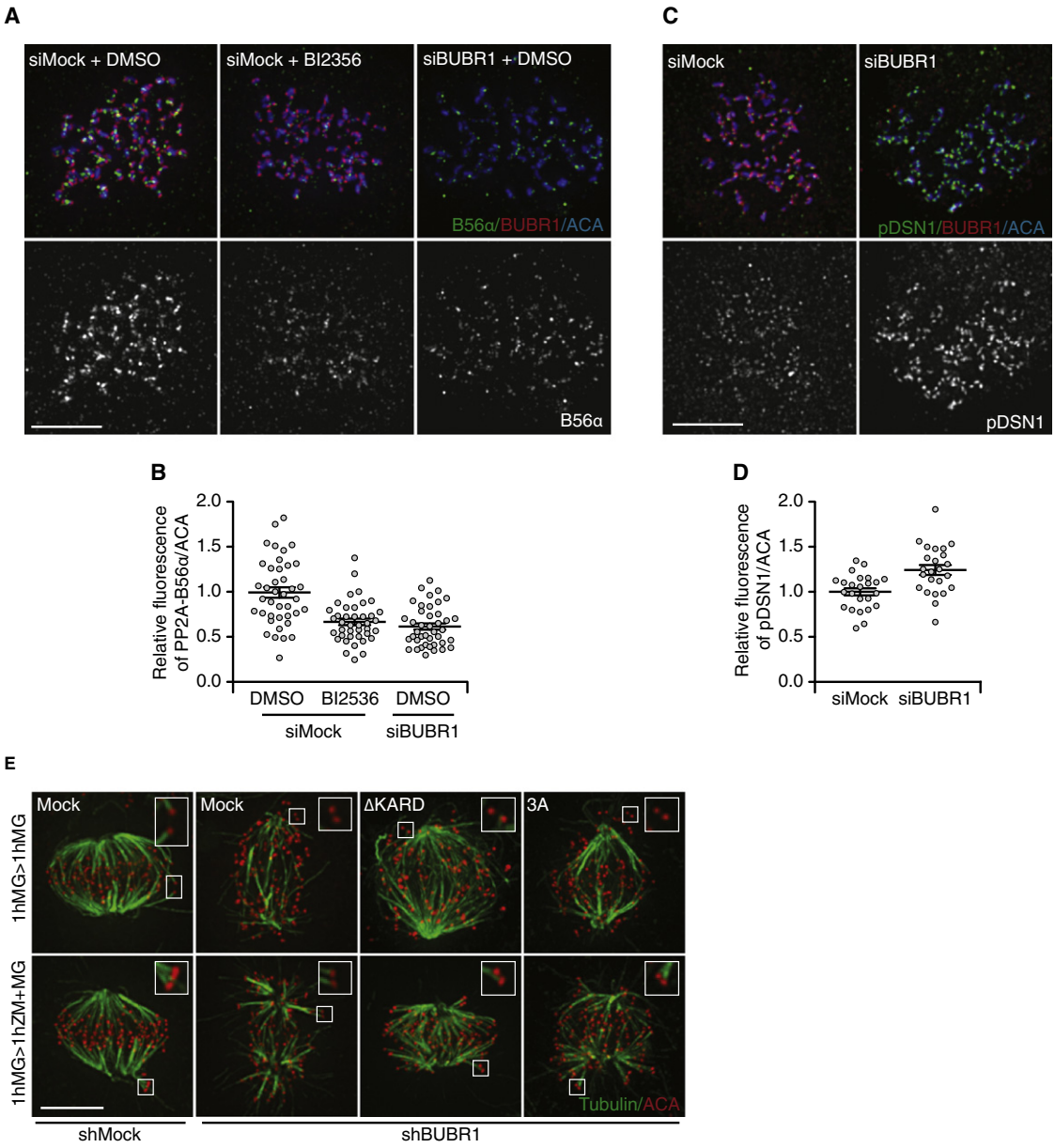

Figure 6. Phospho-KARD Recruits PP2A-B56α to Kinetochores to Counter Excessive Aurora B Activity

(A–D) PP2A-B56α, pS109-DSN1 (pDSN1), and BUBR1 immunolocalization in HeLa cells transfected with indicated siRNAs, treated with nocodazole, MG132, and DMSO or BI2536 for 30 min, and immunostained for PP2A-B56α (A and B) or pDSN1 (C and D), along with BUBR1 and centromeres (ACA). Representative images are shown and graphs represent total kinetochore intensity of PP2A-B56α (B) or pDSN1 (D) relative to centromeres (ACA), ±SD.

(E) Cold-stable microtubules in HeLa cells transfected and treated as indicated, and immunostained for tubulin and centromeres (ACA).

phosphorylated by PLK1. PLK1-dependent regulation of PP2A kinetochore localization via BUBR1 phosphorylation may thus be an important mechanism by which PLK1 controls kinetochore-microtubule attachments (Foley et al., 2011; Lénárt et al., 2007; Sumara et al., 2004; van Vugt et al., 2004) and possibly also microtubule dynamics (Liu et al., 2012). BUBR1 thus couples signaling by PLK1 with regulation of outer-kinetochore phosphorylation by Aurora B. It is of interest to note that besides T620, an additional residue amino-terminal to the KARD was recently shown to be involved in chromosome alignment. Phosphorylation of this T608 partially mediated chromosome alignment by the kinetochore-localized kinesin CENP-E (Guo et al., 2012). T608 is close to the PLK1 binding site in BUBR1 (pT620, (Elowe et al., 2007)) and is within a consensus motif for phosphorylation by PLK1, although it was suggested to be an autophosphorylation site (Guo et al., 2012). Since BUBR1 is a pseudokinase (Suijkerbuijk et al., 2012; Vleugel et al., 2012), T608 might instead be a PLK1 phosphorylation site and it would of interest to examine whether pT608 contributes to PLK1-dependent KARD phosphorylation and PP2A

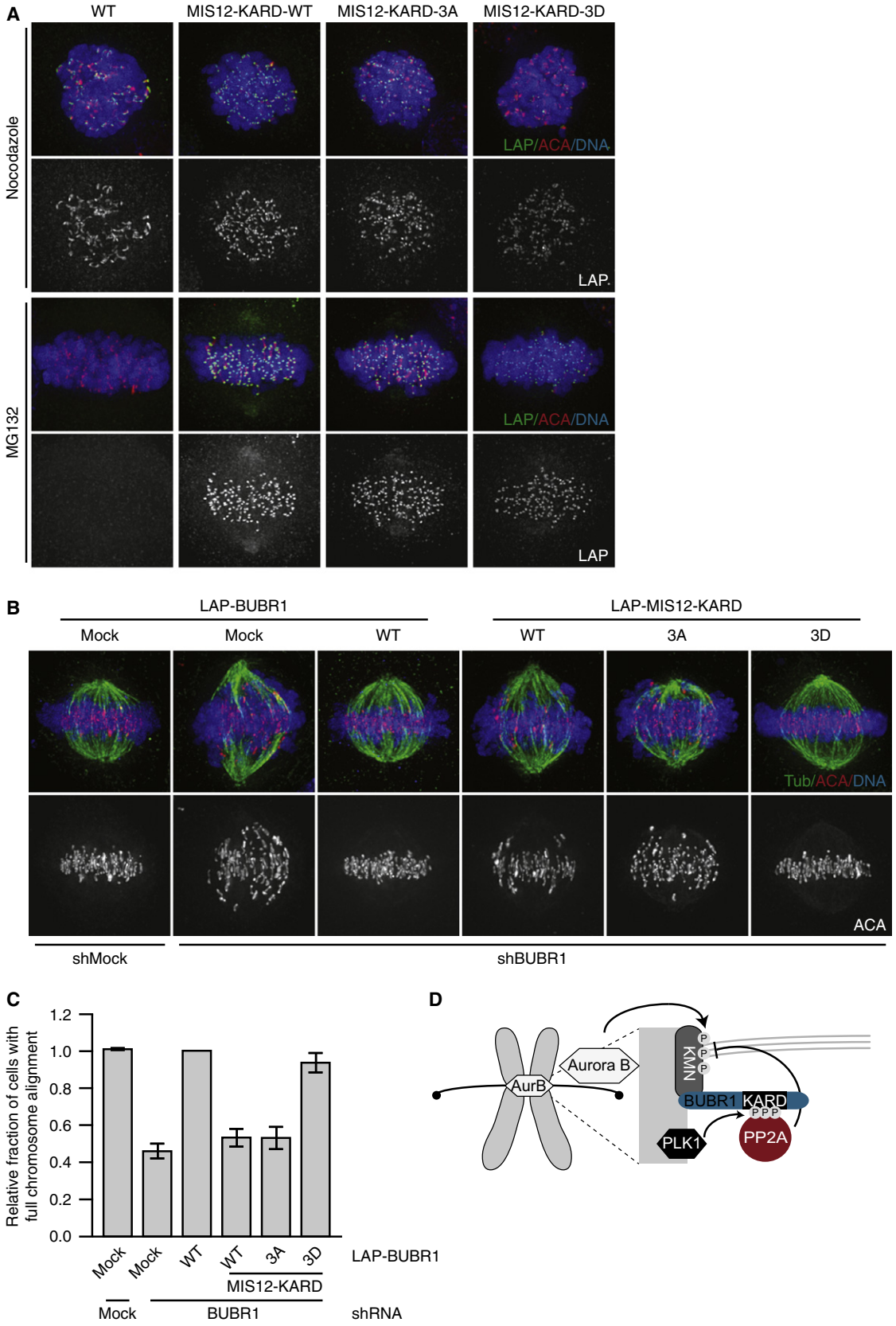
A
WT
MIS12-KARD-WT
MIS12-KARD-3A
MIS12-KARD-3D
Nocodazole
MG132
LAP/ACA/DNA
LAP
B
LAP-BUBR1
LAP-MIS12-KARD
Mock
Mock
WT
WT
3A
3D
Tub/ACA/DNA
ACA
shMock
shBUBR1
C
Relative fraction of cells with full chromosome alignment
1.2
1.0
0.8
0.6
0.4
0.2
0.0
Mock
Mock
WT
WT
3A
3D
LAP-BUBR1
MIS12-KARD
Mock
BUBR1
shRNA
D
AurB
Aurora B
KMN
BUBR1
KARD
PLK1
PP2A

kinetochore binding, and whether this may explain its involvement in the regulation of chromosome alignment by CENP-E.

A recent structure of the PP2A AB′C holoenzyme in complex with parts of the SGO1 homodimer revealed how SGO1 directly interacts with the B and C subunits of PP2A (Xu et al., 2009). Critical residues in the interaction between B56 and SGO1 are L83, K87, and Y90 that somewhat resemble the **I**EDS**R**EA**T**H sequence in the KARD of BUBR1. Although the recruitment of PP2A to BUBR1-decorated LacO foci is suggestive, it is unclear whether BUBR1 can directly interact with PP2A-B56α or how phosphorylation of the three residues in the KARD may contribute to the putative interaction. It will be of interest to investigate whether the KARD represents a similar PP2A interaction site as the one found in SGO1. In vitro binding studies of the PP2A holoenzyme with the KARD-containing region of BUBR1 may provide conclusive insight into this important question.

Chromosome biorientation is a complex process, which likely requires multiple layers of feedback control to fine-tune the balance between stabilization and destabilization of kinetochore-microtubule attachments, in order to allow efficient and error-free segregation of chromosomes. The data presented here place BUBR1 as an integrator of such balancing signals, and imply extensive feedbacks in the PLK1-BUBR1-PP2A-Aurora B module. While BUBR1 depends on Aurora B activity for its localization to unattached kinetochores (Ditchfield et al., 2003), it may, in turn, indirectly contribute to removal of these phosphoresidues. Moreover, localized activity of PLK1, the kinase responsible for phosphorylation of the KARD domain, is kept in balance by PP2A-B56 that regulates PLK1 kinetochore binding (Foley et al., 2011). Although paradoxical at first glance, these feedback likely fine-tune relative levels of kinase-phosphatase activities at kinetochores and may be interrupted by deformations of the centromere and kinetochore, such as those imposed by bioriented attachments (Suzuki et al., 2011; Wan et al., 2009). Moreover, BUBR1 recruitment to kinetochores depends on lack of tension between sister chromatids (Skoufias et al., 2001). Removal of BUBR1, and thereby PP2A-B56, upon establishment of stable microtubule-kinetochore attachments will allow a switch to the metaphase Aurora B-counteracting phosphatase PP1γ (Liu et al., 2010). Thorough examinations of these and other feedback will be crucial to our understanding of how chromosomes establish, correct, and maintain stable interactions between kinetochores and spindle microtubules.

EXPERIMENTAL PROCEDURES

Cell Culture, Plasmids, and Transfections

HeLa, HEK293T and U2OS cells were grown in DMEM supplemented with 8% fetal bovine serum and penicillin/streptomycin (50 μg/ml). The U2OS LacO cell line (a gift from S. Janicki) was grown in the presence of 100 μg/ml hygromycin B.

pSuper-Mock (Jelluma et al., 2008), pSuper-BUBR1 (Kops et al., 2004), pLAP-BUBR1 (Suijkerbuijk et al., 2010), LAP-Mock (Suijkerbuijk et al., 2010), and HA-PP2A-B56α (addgene plasmid 14532) were previously described. LAP-BUBR1 mutants were obtained by site-directed mutagenesis. pLacI-LAP-BUBR1 constructs and mutants were created by a LacI PCR from pKG194 (Gascoigne et al., 2011) (a gift from I. Cheeseman) and subsequent cloning into the Nhe1 site of the pLAP-BUBR1 constructs. LAP-KARD (WT, 3A, and 3D, amino acid 647–697) was generated by PCR on WT or mutant LAP-BUBR1 and subsequent ligation using SalI/BamHI into the XhoI/BamHI sites of pIC58. LAP-MIS12-KARD was cloned by a PCR on full-length Mis12 and subsequent ligation using Xba1 into the Spe1 site of LAP-KARD.

Cells were cotransfected with a pH2B-eYFP marker plasmid along with pSuper-BUBR1 or pSuper-Mock and shRNA-insensitive LAP- BUBR1-WT or mutants in a 1:8:5 ratio using Fugene (HeLa) or $CaPO_4$ (U2OS). The ratio was based on the functional rescue by wild-type in relation to the shRNA. U2OS LacO cells were cotransfected with pLacI-LAP-BUBR1 and HA-PP2A-B56α in a 1:1 ratio in the presence of 1 mM isopropyl β-D-thiogalactoside (IPTG), using fugene.

siRNAs used in this study were as follows: siMock (Luciferase GL2 duplex; Dharmacon/D-001100-01-20), siBUBR1 (5′-AAAGAUCCUGGCUAACUGUUC-3′, custom Ambion). All siRNAs were transfected using Hiperfect (QIAGEN) at 20 nM according to the manufacturer's instructions.

Thymidine (2.5 mM, Sigma), Nocodazole (250 ng/ml, Sigma), MG132 (5 μM, Sigma), ZM447439 (2 μM, Tocris Bioscience), BI2536 (100 nM, Boehringer Ingelheim Pharma), and IPTG (1 mM, Fermentas).

Immunofluorescence

HeLa and U2OS LacO cells were plated, transfected on 12 mm coverslips, and treated as described in figure legends. For kinetochore staining, kinetochore-staining cells were pre-extracted with PEM/TX (100 mM PIPES [pH 6.8], 1 mM $MgCl_2$, 5 mM EGTA, 0.2% Triton X-100) for 1 min before a 5 min fixation in 3.7% formaldehyde in PEM/TX. For tubulin staining, cells were fixed while permeabilizing for 15 min in 3.7% Shandon Zinc Formal-Fixx (Thermo Scientific) in PEM/TX, with a 15 min cold treatment prior to fixation for analysis of cold-stable microtubules. Coverslips were blocked with 3% BSA in PBS for 1 hr, incubated with primary antibody for 16 hr at 4°C, washed with PBS/0.1% Triton X-100, and incubated with secondary antibodies for an additional 1 hr at room temperature. Coverslips were washed and submerged in PBS containing DAPI and mounted using ProLong Gold antifade (Molecular Probes). Image acquisition and quantification were done as described (Saurin et al., 2011), using a DeltaVision RT system (Applied Precision) with a 100×/1.40 numerical aperture (NA) UPlanSApo objective (Olympus) for acquiring images, ImageJ software for quantification and Photoshop CS5 (Adobe) for image processing.

Immunoprecipitation and Immunoblotting

HEK 293T cells transfected with LAP-BUBR1 and HA-PP2A-B56α, were treated with nocodazole for 18 hr (Figure 5B), or HeLa cells untransfected (Figure 3C) or transfected with LAP-BUBR1 (Figures 3B and 4B) were released from a 24 hr thymidine-induced block into the indicated spindle poison followed for 16 hr, followed by BI2536 treatment for 1 hr (Figure 4B). Cells were lysed in lysis buffer (50 mM HEPES [pH 7.5], 150 mM NaCl, 5 mM EDTA, 0.5% NP-40, 1 mM Na3VO4, 1 mM β-glycerophosphate, 1 mM NaF, and complete protease inhibitor [Roche]). Endogenous BUBR1 was bound to G protein-agarose (Roche) with anti-BUBR1 (Custom sheep polyclonal) and LAP-BUBR1 was bound to S protein-agarose (Novagen) for 2 hr, washed four times in lysis buffer, after removal of all buffer, sample buffer was added or for phosphatase treatment (Figure 3B) were incubated in lambda phosphatase buffer (NEB) containing Mn^{2+} in the presence or absence of lambda

Figure 7. Phospho-KARD Is Sufficient for Formation of Kinetochore-Microtubule Interactions by BUBR1

(A) BUBR1 localization in HeLa cells transfected with LAP-BUBR1-WT or LAP-MIS12-KARD (WT or mutant), treated with nocodazole and MG132 for 1 hr, and immunostained for GFP and centromeres (ACA).

(B and C) Chromosome alignment in HeLa cells transfected with indicated shRNAs in combination with RNAi-insensitive LAP-tagged BUBR1 and treated with MG132 for 1 hr and immunostained for tubulin and centromeres (ACA). Representative images are shown (B) and graph (C) represents the relative fraction of cells with full chromosome alignment (average of three experiments, ±SEM).

(D) Model depicting the regulation of kinetochore-microtubule attachments by cooperation of PLK1 and BUBR1. Phosphorylation of BUBR1 by PLK1 at kinetochores regulates PP2A-B56-mediated dephosphorylation of Aurora B substrates.

phosphatase (NEB) at 30 min at 37°C, followed by addition of sample buffer. Samples were separated by SDS-PAGE. Immunoblotting was done using standard protocols; the signal was visualized and analyzed on an Odyssey scanner (LI-COR Biosciences) using fluorescently labeled secondary antibodies (Figures 1B, 3B, 3C, 4B, and 5B) or was detected by using enhanced chemiluminescence (Figures 3B, 3C, 4A, and 5B).

PLK1 Kinase Assay

LAP-BUBR1 substrate was purified from thymidine treated HEK 293T cells, by lysis in lysis buffer (50 mM HEPES [pH 7.5], 150 mM NaCl, 5 mM EDTA, 0.5% NP-40, 1 mM Na_3VO_4, 1 mM β-glycerophosphate, 1 mM NaF and complete protease inhibitor [Roche]). Followed by binding to S protein-agarose (Novagen) for 2 hr, washing four times in lysis buffer and two times in kinase buffer (20 mM HEPES [pH 7.5], 130 mM KCl, 10 mM MgCl, 1 mM EGTA, 1 mM Na_3VO_4, 1 mM β-glycerophosphate, 1 mM NaF, 1 mM DTT). Dried beads were incubated 30 min at 37°C with recombinant PLK1 WT or K82R in 30 μl reactions containing; 100 μM ATP in kinase buffer supplemented with 100 nM BI2536 or DMSO. Reactions were stopped by addition of sample buffer and incubation at 95°C.

Yeast Two-Hybrid

For the ULTImate Y2H screen (performed by Hybrigenics), the bait, human BUBR1 fragment amino acid 540–1050 (with kinase dead mutation, K795A), was tested on a Human Breast Tumor Epithelial Cells RP1 cDNA prey library.

Antibodies

The pT680-BUBR1 antibody was raised in rabbits using the peptide REA-pT-HSSGFSGSSAKKC coupled to KLH as antigen and affinity purified using the described peptide (Covance). The antibody was used in the presence of nonphosphorylated peptide (1 ng/ml) in all experiments.

The antibodies used in this study were α-Tubulin (Sigma, Cat# T5168), green fluorescent protein (GFP) (custom rabbit polyclonal), BUBR1 (Bethyl, Cat# A300-386A), BUBR1 (custom sheep polyclonal), pDSN1 pS109 (gift from I. Cheeseman [Welburn et al., 2010]), PP2A-B56α (BD Trans lab, Cat# 610615), HA-probe Y-11 (Santa Cruz, Cat# sc-805), and HA-probe (custom monoclonal 12CA5).

ACKNOWLEDGMENTS

We are grateful to R. van Heesbeen, N. Hubner, V. Groenewold, and L. Kleij for technical assistance; to I. Cheeseman, K. Gascoigne, and S. Janicki for reagents; to A. Saurin, N. Jelluma, and S. Lens for valuable suggestions and critical reading of the manuscript; and to the Kops, Lens, and Medema laboratories for valuable discussions. This work was supported by the Dutch Cancer Society (KWF UU-2009-4516) and the European Research Council (ERC-StG KINSIGN).

Received: May 9, 2012
Revised: August 22, 2012
Accepted: September 11, 2012
Published online: October 15, 2012

REFERENCES

Alexander, J., Lim, D., Joughin, B.A., Hegemann, B., Hutchins, J.R.A., Ehrenberger, T., Ivins, F., Sessa, F., Hudecz, O., Nigg, E.A., et al. (2011). Spatial exclusivity combined with positive and negative selection of phosphorylation motifs is the basis for context-dependent mitotic signaling. Sci. Signal. *4*, ra42.

Cheeseman, I.M., Chappie, J.S., Wilson-Kubalek, E.M., and Desai, A. (2006). The conserved KMN network constitutes the core microtubule-binding site of the kinetochore. Cell *127*, 983–997.

DeLuca, J.G., Gall, W.E., Ciferri, C., Cimini, D., Musacchio, A., and Salmon, E.D. (2006). Kinetochore microtubule dynamics and attachment stability are regulated by Hec1. Cell *127*, 969–982.

Ditchfield, C., Johnson, V.L., Tighe, A., Ellston, R., Haworth, C., Johnson, T., Mortlock, A., Keen, N., and Taylor, S.S. (2003). Aurora B couples chromosome alignment with anaphase by targeting BubR1, Mad2, and Cenp-E to kinetochores. J. Cell Biol. *161*, 267–280.

Elowe, S., Hümmer, S., Uldschmid, A., Li, X., and Nigg, E.A. (2007). Tension-sensitive Plk1 phosphorylation on BubR1 regulates the stability of kinetochore microtubule interactions. Genes Dev. *21*, 2205–2219.

Elowe, S., Dulla, K., Uldschmid, A., Li, X., Dou, Z., and Nigg, E.A. (2010). Uncoupling of the spindle-checkpoint and chromosome-congression functions of BubR1. J. Cell Sci. *123*, 84–94.

Foley, E.A., Maldonado, M., and Kapoor, T.M. (2011). Formation of stable attachments between kinetochores and microtubules depends on the B56-PP2A phosphatase. Nat. Cell Biol. *13*, 1–8.

Gascoigne, K.E., Takeuchi, K., Suzuki, A., Hori, T., Fukagawa, T., and Cheeseman, I.M. (2011). Induced ectopic kinetochore assembly bypasses the requirement for CENP-A nucleosomes. Cell *145*, 410–422.

Guo, Y., Kim, C., Ahmad, S., Zhang, J., and Mao, Y. (2012). CENP-E-dependent BubR1 autophosphorylation enhances chromosome alignment and the mitotic checkpoint. J. Cell Biol. *198*, 205–217.

Huang, H., Hittle, J., Zappacosta, F., Annan, R.S., Hershko, A., and Yen, T.J. (2008). Phosphorylation sites in BubR1 that regulate kinetochore attachment, tension, and mitotic exit. J. Cell Biol. *183*, 667–680.

Janicki, S.M., Tsukamoto, T., Salghetti, S.E., Tansey, W.P., Sachidanandam, R., Prasanth, K.V., Ried, T., Shav-Tal, Y., Bertrand, E., Singer, R.H., and Spector, D.L. (2004). From silencing to gene expression: real-time analysis in single cells. Cell *116*, 683–698.

Janssens, V., and Goris, J. (2001). Protein phosphatase 2A: a highly regulated family of serine/threonine phosphatases implicated in cell growth and signalling. Biochem. J. *353*, 417–439.

Jelluma, N., Brenkman, A.B., van den Broek, N.J., Cruijsen, C.W., van Osch, M.H., Lens, S.M., Medema, R.H., and Kops, G.J. (2008). Mps1 phosphorylates Borealin to control Aurora B activity and chromosome alignment. Cell *132*, 233–246.

Jelluma, N., Dansen, T.B., Sliedrecht, T., Kwiatkowski, N.P., and Kops, G.J.P.L. (2010). Release of Mps1 from kinetochores is crucial for timely anaphase onset. J. Cell Biol. *191*, 281–290.

Kapoor, T.M., Mayer, T.U., Coughlin, M.L., and Mitchison, T.J. (2000). Probing spindle assembly mechanisms with monastrol, a small molecule inhibitor of the mitotic kinesin, Eg5. J. Cell Biol. *150*, 975–988.

Kitajima, T.S., Sakuno, T., Ishiguro, K.-I., Iemura, S.-I., Natsume, T., Kawashima, S.A., and Watanabe, Y. (2006). Shugoshin collaborates with protein phosphatase 2A to protect cohesin. Nature *441*, 46–52.

Kops, G.J.P.L., Foltz, D.R., and Cleveland, D.W. (2004). Lethality to human cancer cells through massive chromosome loss by inhibition of the mitotic checkpoint. Proc. Natl. Acad. Sci. USA *101*, 8699–8704.

Lampson, M.A., and Kapoor, T.M. (2005). The human mitotic checkpoint protein BubR1 regulates chromosome-spindle attachments. Nat. Cell Biol. *7*, 93–98.

Lénárt, P., Petronczki, M., Steegmaier, M., Di Fiore, B., Lipp, J.J., Hoffmann, M., Rettig, W.J., Kraut, N., and Peters, J.-M. (2007). The small-molecule inhibitor BI 2536 reveals novel insights into mitotic roles of polo-like kinase 1. Curr. Biol. *17*, 304–315.

Liu, D., Vader, G., Vromans, M.J.M., Lampson, M.A., and Lens, S.M.A. (2009). Sensing chromosome bi-orientation by spatial separation of aurora B kinase from kinetochore substrates. Science *323*, 1350–1353.

Liu, D., Vleugel, M., Backer, C.B., Hori, T., Fukagawa, T., Cheeseman, I.M., and Lampson, M.A. (2010). Regulated targeting of protein phosphatase 1 to the outer kinetochore by KNL1 opposes Aurora B kinase. J. Cell Biol. *188*, 809–820.

Liu, D., Davydenko, O., and Lampson, M.A. (2012). Polo-like kinase-1 regulates kinetochore-microtubule dynamics and spindle checkpoint silencing. J. Cell Biol. *198*, 491–499.

Maldonado, M., and Kapoor, T.M. (2011). Constitutive Mad1 targeting to kinetochores uncouples checkpoint signalling from chromosome biorientation. Nat. Cell Biol. *13*, 475–482.

Malureanu, L.A., Jeganathan, K.B., Hamada, M., Wasilewski, L., Davenport, J., and van Deursen, J.M. (2009). BubR1 N terminus acts as a soluble inhibitor of cyclin B degradation by APC/C(Cdc20) in interphase. Dev. Cell *16*, 118–131.

Nakajima, H., Toyoshima-Morimoto, F., Taniguchi, E., and Nishida, E. (2003). Identification of a consensus motif for Plk (Polo-like kinase) phosphorylation reveals Myt1 as a Plk1 substrate. J. Biol. Chem. *278*, 25277–25280.

Riedel, C.G., Katis, V.L., Katou, Y., Mori, S., Itoh, T., Helmhart, W., Gálová, M., Petronczki, M., Gregan, J., Cetin, B., et al. (2006). Protein phosphatase 2A protects centromeric sister chromatid cohesion during meiosis I. Nature *441*, 53–61.

Saurin, A.T., van der Waal, M.S., Medema, R.H., Lens, S.M.A., and Kops, G.J.P.L. (2011). Aurora B potentiates Mps1 activation to ensure rapid checkpoint establishment at the onset of mitosis. Nat. Commun. *2*, 316.

Skoufias, D.A., Andreassen, P.R., Lacroix, F.B., Wilson, L., and Margolis, R.L. (2001). Mammalian mad2 and bub1/bubR1 recognize distinct spindle-attachment and kinetochore-tension checkpoints. Proc. Natl. Acad. Sci. USA *98*, 4492–4497.

Suijkerbuijk, S.J.E., van Osch, M.H.J., Bos, F.L., Hanks, S., Rahman, N., and Kops, G.J.P.L. (2010). Molecular causes for BUBR1 dysfunction in the human cancer predisposition syndrome mosaic variegated aneuploidy. Cancer Res. *70*, 4891–4900.

Suijkerbuijk, S.J.E., van Dam, T.J.P., Karagöz, G.E., von Castelmur, E., Hubner, N.C., Duarte, A.M.S., Vleugel, M., Perrakis, A., Rüdiger, S.G.D., Snel, B., and Kops, G.J. (2012). The vertebrate mitotic checkpoint protein BUBR1 is an unusual pseudokinase. Dev. Cell *22*, 1321–1329.

Sumara, I., Giménez-Abián, J.F., Gerlich, D., Hirota, T., Kraft, C., de la Torre, C., Ellenberg, J., and Peters, J.M. (2004). Roles of polo-like kinase 1 in the assembly of functional mitotic spindles. Curr. Biol. *14*, 1712–1722.

Suzuki, A., Hori, T., Nishino, T., Usukura, J., Miyagi, A., Morikawa, K., and Fukagawa, T. (2011). Spindle microtubules generate tension-dependent changes in the distribution of inner kinetochore proteins. J. Cell Biol. *193*, 125–140.

Tang, Z., Shu, H., Qi, W., Mahmood, N.A., Mumby, M.C., and Yu, H. (2006). PP2A is required for centromeric localization of Sgo1 and proper chromosome segregation. Dev. Cell *10*, 575–585.

van Vugt, M.A.T.M., van de Weerdt, B.C.M., Vader, G., Janssen, H., Calafat, J., Klompmaker, R., Wolthuis, R.M.F., and Medema, R.H. (2004). Polo-like kinase-1 is required for bipolar spindle formation but is dispensable for anaphase promoting complex/Cdc20 activation and initiation of cytokinesis. J. Biol. Chem. *279*, 36841–36854.

Vleugel, M., Hoogendoorn, E., Snel, B., and Kops, G.J.P.L. (2012). Evolution and function of the mitotic checkpoint. Dev. Cell *23*, 239–250.

Wan, X., O'Quinn, R.P., Pierce, H.L., Joglekar, A.P., Gall, W.E., DeLuca, J.G., Carroll, C.W., Liu, S.-T., Yen, T.J., McEwen, B.F., et al. (2009). Protein architecture of the human kinetochore microtubule attachment site. Cell *137*, 672–684.

Waters, J.C., Chen, R.H., Murray, A.W., and Salmon, E.D. (1998). Localization of Mad2 to kinetochores depends on microtubule attachment, not tension. J. Cell Biol. *141*, 1181–1191.

Wei, R.R., Al-Bassam, J., and Harrison, S.C. (2007). The Ndc80/HEC1 complex is a contact point for kinetochore-microtubule attachment. Nat. Struct. Mol. Biol. *14*, 54–59.

Welburn, J.P.I., Vleugel, M., Liu, D., Yates, J.R., 3rd, Lampson, M.A., Fukagawa, T., and Cheeseman, I.M. (2010). Aurora B phosphorylates spatially distinct targets to differentially regulate the kinetochore-microtubule interface. Mol. Cell *38*, 383–392.

Xu, Z., Cetin, B., Anger, M., Cho, U.S., Helmhart, W., Nasmyth, K., and Xu, W. (2009). Structure and function of the PP2A-shugoshin interaction. Mol. Cell *35*, 426–441.